JOURNAL OF MATERIALS SCIENCE **36** (2001) 429–439

Interfacial reactions in an Al-Cu-Mg (2009)/SiC*w* composite during liquid processing

Part II *Arc welding*

A. UREÑA*, P. RODRIGO, L. GIL
Dept. Ciencias Experimentales e Ingeniería, Escuela Superior de Ciencias Experimentales y Tecnología, Universidad Rey Juan Carlos, 28933 Móstoles, Madrid, Spain
E-mail: a.urena@escet.urjc.es

M. D. ESCALERA
Dept. Ciencia de los Materiales e Ingeniería Metalúrgica, Facultad de Ciencias Químicas, Universidad Complutense de Madrid, 28040 Madrid, Spain

J. L. BALDONEDO
Centro de Microscopía Electrónica "Luis Bru", Universidad Complutense de Madrid, 28040 Madrid, Spain

This paper reports a study of the interfacial reactions occurring in an aluminium alloy composite (AA2009) reinforced with 15% volume in SiC whiskers, under high energy fusion conditions. The composite was subjected to melting processes that simulated a secondary composite manufacture technique such as arc welding. The different reaction mechanisms between the SiC whiskers and both the molten aluminium and their alloying elements (Cu, Mg, and Fe) are discussed. The high aspect ratio (*l*/*d*) of the reinforcement is the main microstructural factor, which controls the weldability of this kind of composite, having more influence than the actual interfacial reactivity. Under the highest welding inputs applied, the formation of both a binary aluminium carbide (Al_4C_3) and a ternary one (β-Al_4SiC_4) was detected in the top of the molten pools. It is observed that these ternary carbides are harder and more chemically stable than the Al_4C_3, which is formed at lower temperatures.

1. Introduction

Despite the potential advantages of using aluminium matrix composites (AMC) for structural applications, they are not yet widely used in industry. This is due to several limitations, which are associated with the unsuitable application of many of the conventional manufacturing processes used for unreinforced aluminium alloys. Welding is one of the more important of these problems, especially when fusion of the composite materials is required. The fabrication of any complex structure with structural functions requires strong and durable joints, and the presence of the reinforcement component in the aluminium matrix would necessarily affect both the performance of the welding procedure and the properties of the joint.

From previous studies carried out by the present authors [1, 2] or other investigators [3, 4] it can be deduced that, in general, AMCs show poor weldability when fusion welding methods are used. These weldability problems are especially important when it is attempted to weld reactive systems (Al-SiC, Al-C, etc) by high energy fusion methods such as arc welding [5], electron beam [3] or laser [6]. Most of this literature refers to the welding of aluminium alloys reinforced with different proportions of SiC particles, applying Si-rich Al alloys as fillers (i.e. 4047) [7] to avoid interfacial reaction between SiC and molten aluminium. This reaction has been well documented [8, 9] not only in welding but also during casting. It occurs as follows:

$$3SiC_{(s)} + 4Al_{(l)} \rightarrow Al_4C_{3(s)} + 3Si_{(Al)} \qquad (1)$$

The free energy change for the reaction [10] is:

$$\Delta G\,(\mathrm{J/mol}) = 113.900 - 12.06T \times \ln T + 8.92 \times 10^{-3}T^2 + 7.35 \times 10^{-4}T^{-1} + 21.5T + RT \times \ln a_{[Si]} \qquad (2)$$

where $a_{[Si]}$ is the activity of free Si in liquid Al, R the gas constant and T the absolute temperature.

Apart from using Al-Si fillers, the other way to avoid this reaction is to weld with minimum superheating in order to reduce the time and temperature of contact between SiC and molten Al. Aluminium alloys of both

* Author to whom all correspondence should be addressed.

2××× and 7××× series [11], reinforced with SiC particles, have been autogenous TIG (Tungsten Inert Gas) welded using low arc energies.

However, there are no data enough on fusion welding of AMCs reinforced with SiC whiskers, which are defect-free monocrystalline reinforcements with high aspect ratios. The structure and special shape of this kind of ceramic reinforcements play an important role in the interfacial reactions which occur when molten aluminium comes into contact with them. Under the high energy conditions characteristic of arc welding, the reaction mechanisms are not stabilised, and it would therefore be useful to ascertain the influence of these on the composite microstructure.

This second part of the paper reports in detail on the reaction mechanisms between SiC whiskers and

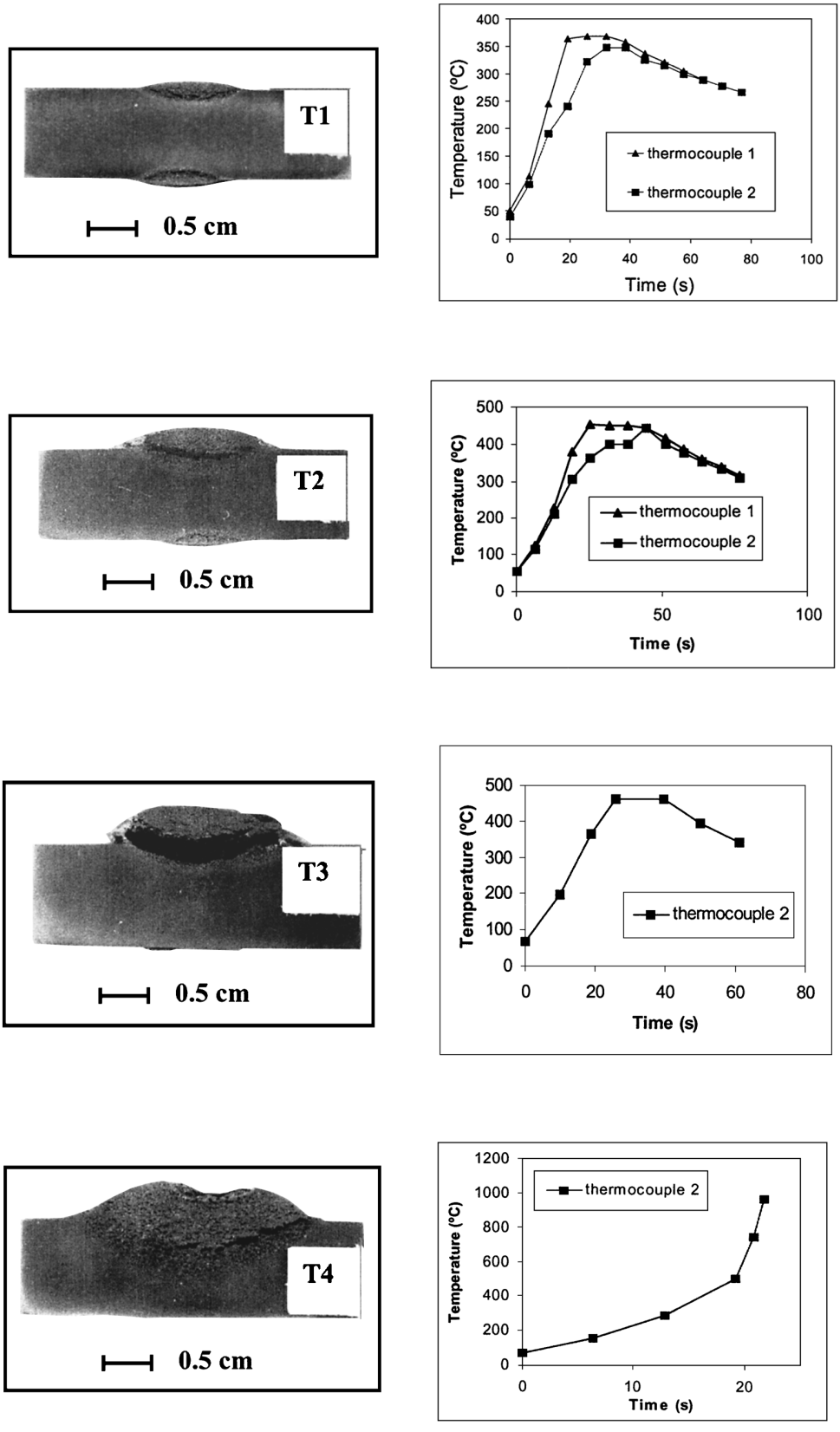

Figure 1 Macrographies of the TIG welding tests applied on the composite sheets. Temperature cycles for each weld (measured with thermocouples located at 8 and 13 mm from the weld axis).

TABLE I TIG welding conditions applied on the composite specimens

TEST N.	T1		T2		T3		T4
Conditions	*Weld 1*	*Weld 2*	*Weld 1*	*Weld 2*	*Weld 1*	*Weld 2*	*Weld 1*
I_0 (A)	100	115	125	125	150	150	175
I (A)	111	123	131	131	150	150	170
V (V)	16.6	16.8	17.1	16.8	17.1	16.9	17.9
P (W)	1843	2066	2240	2200	2565	2535	3050

I_0 = initial intensity I = average intensity V = voltage P = weld-break ing power.

an Al-Cu-Mg (2009) alloy under different arc melting conditions. For this study, light (LM), scanning (SEM) and transmission electron microscopies (TEM) were applied along with electron diffraction (ED) and other structural and microanalytical techniques (XRD and EDX) which made it possible to identify the interface products formed. A comparative study with the mechanisms of interfacial reaction identified for casting conditions in the first part of this work was also established. The effect of the interfacial reaction on the fracture mechanisms is also reported.

2. Experimental procedure

2.1. Parent composite

The composite material used for the present investigation was an aluminium alloy 2009 reinforced with 15 percent volume of SiC whiskers. Its composition and reception characteristics are described in the first part of this paper.

2.2. Reaction tests by matrix controlled welding

To study the reactivity between SiC whiskers and AA2009 matrix alloy when in molten phase under a welding procedure, simulated TIG arc fusion tests were applied. These were done on $76 \times 40 \times 9$ mm blanks machined from the parent plate, using a TIG (Tungsten Inert Gas) welding machine (ARISTO TIG-250). Two molten pools were generated on each side of the tested specimens, applying different input power. For one specimen only, a single-side weld was applied at the higher power. All welding tests were carried out using pure argon (99.999%) as protective atmosphere with a flow rate of 9.5 l/min. The arc discharge and its displacement on the specimen surface were produced automatically using a *Bugo* system at a constant welding speed (100 mm/min). The welding conditions for each test are shown in Table I. Temperatures were registered by thermocouples located 8 and 13 mm respectively from the arc discharge line.

2.3. Characterisation studies

Cross sections of the welded specimens were characterised by light microscopy (LM), scanning electron microscopy (SEM) (JEOL-35C, JEOL-6400) and transmission electron microscopy (JEOL 2000 FX-200 kV). The interface microstructure was examined using bright field (BF) and dark field (DF) images, electron difraction (ED) and energy dispersive X-ray spectroscopy (EDX). Prior to these studies, bulk structural changes in the composite under the different testing conditions were monitored by X-ray diffraction (XRD) using a Cu anti-cathode (Kα Cu = 1.5405 Å). For the specimen welded at higher input power, four slices approximately 2 mm thick were cut parallel to the welding surface in order to study the evolution in microstructure with the distance from the arc discharge line.

The TEM thin foils were prepared by ion milling at 5 kV and 1 mA, keeping the temperature at 20 °C and using an Ar^+ beam with an incidence angle of 15°. Specimens had previously been mechanically polished and dimpled. All the polishing and grinding operations were done using ethylene glycol as lubricant to avoid the water degradation of the reaction products.

3. Results

3.1. Macrostructural study of arc welds

Post-solidification observation of the molten pools generated on the composite sheets showed the existence of serious wettability problems between the ceramic and metallic constituents. This poor wettability and the accumulation of SiC whisker in the solidification fronts originated a high level of porosity and also hot cracking,

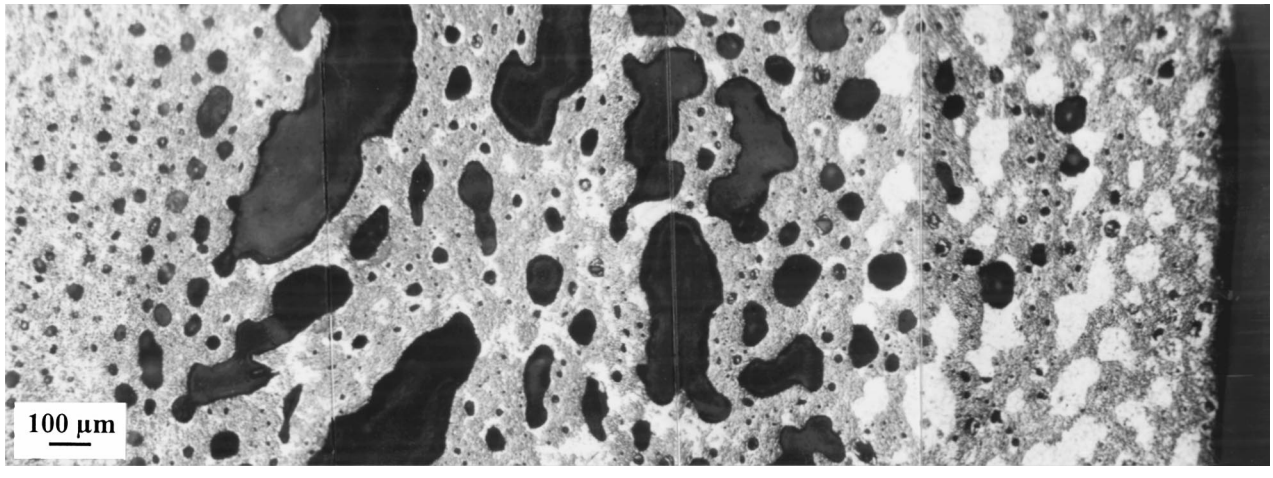

Figure 2 Light micrography of the composite weld showing different zones with changing microstructure.

as shown in cross-sections of the welds (Fig. 1). Fig. 1 also shows the thermal cycles measured during the arc discharge on the top surface at 8 and 13 mm from the weld axis. The temperature attained is a function of the welding power, and heating and cooling rates of approximately 20 and 45 °C respectively were calculated.

LM observation at low magnifications showed a weld structure comprising several zones (Fig. 2), whose width and microstructure depend on welding power. Three zones are usually distinguished:

– zone 1: this is at the top of the weld and is practically free of porosity.
– zone 2: this is in the middle, covering most of the weld, and is characterised by large voids (>100 μm); hot cracking may occasionally appear in this area.
– zone 3: this is at the bottom of the weld, limited by the melting line, where there is homogeneous porosity with sizes of less than 10 μm.

The observations of specimens tested at different powers showed that an increase in the energy used increased the overall penetration of the molten bath, increasing the depth of each of these zones.

To identify the microstructural changes occurring inside these zones, the specimen welded at the highest energy was cut as described in the previous section. XRD was performed on each of these zones. Comparative results are given in Fig. 3. These show that on the surfaces of the slices cut at 9 and 6.5 mm from the top weld surface, the only phases present are the original constituents of the parent composite (Al and α-SiC). However, at 3 mm from the point where the arc was discharged, there are the first signs of formation of Si and Al_4C_3. From the XRD pattern taken from the weld top, where the maximum temperature was attained, the signal corresponding to SiC has disappeared; the height of the Si and Al_4C_3, has increased, and there are new signals which were identified as Al_4SiC_4.

To confirm the formation of those reaction products and of others present in lower proportions, a complete microscopic characterisation of each slice of the solidified pool was carried out using SEM and TEM-DE.

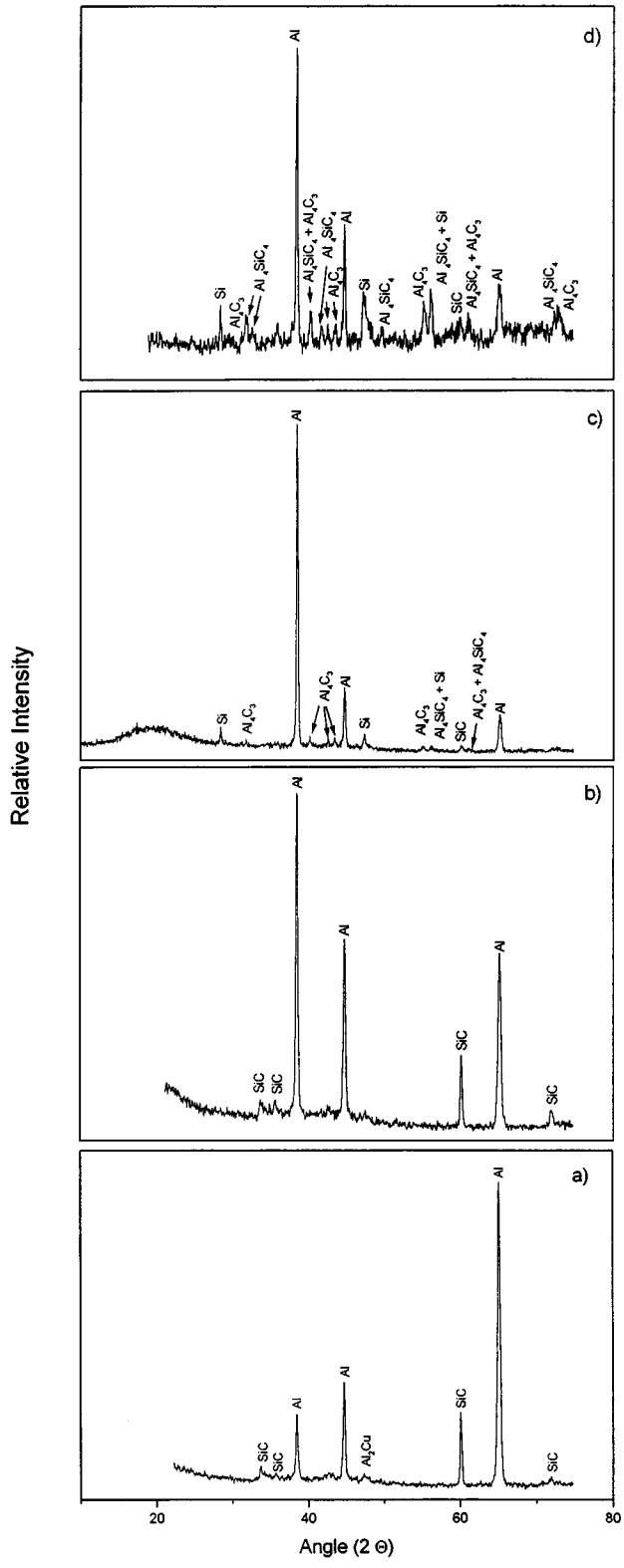

Figure 3 XRD patterns of four slides cut from the previous weld. (a) parent material/fusion zone; (b) weld pool (6.5 mm from the top); (c) weld pool (3 mm from the top); (d) top of the weld.

3.2. Microstructural characterisation

Fig. 4a and b show the microstructure of the solidified pool at 9 mm from the welding surface. Both the redistribution and the formation of porosity in zones of whisker accumulation are apparent. At higher magnifications, SiC whiskers continue to present their original hexagonal cross-sections, and there is no sign of Al_4C_3 formation, although some aggregates of intermetallic rich in copper were detected (marked with arrows). Closer to the arc discharge surface (approx. 6.5 mm), there is an increase in the size and proportion of the porosity, accompanied by re-distribution of the whiskers around the voids. Fig. 5a shows a SEM image corresponding to one of these whisker accumulation zones where their cross-section appears more rounded and many of them are joined together to form continuous structures. The backscattered image (Fig. 5b) reveals the existence of a heavier phase among them, which is probably the Si produced by the reaction (1).

Just under the top of the weld (approximately 3.5 mm away), partial consumption of the SiC whiskers is apparent; there are also extended whisker-free aluminium zones where Si-rich eutectic aggregates are predominant (Fig. 6). Whiskers have been pushed out by the solidification front and appear accumulated around the

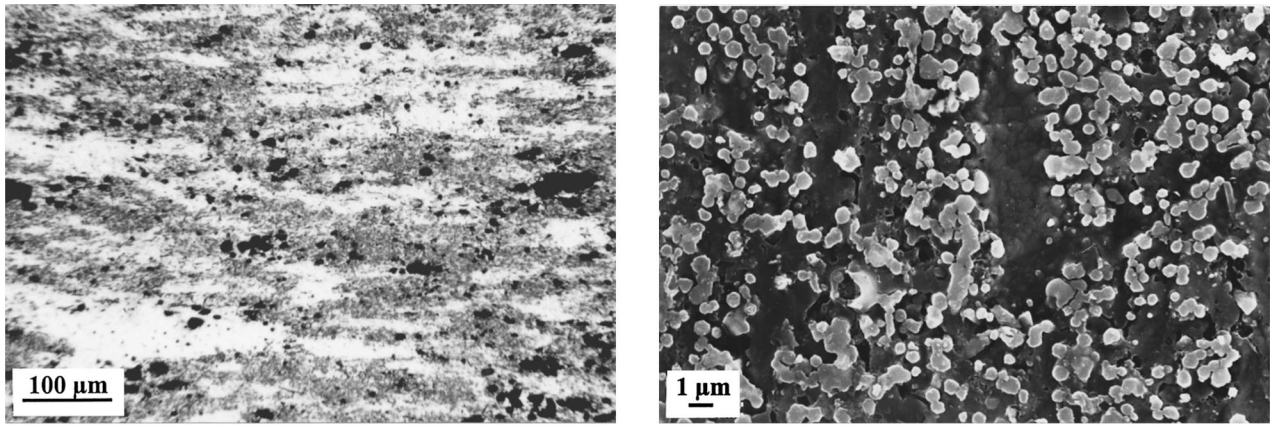

Figure 4 (a) Microstructure of the limit between melting pool and parent composite. (b) SEM detail showing the original hexagonal cross section of the whiskers.

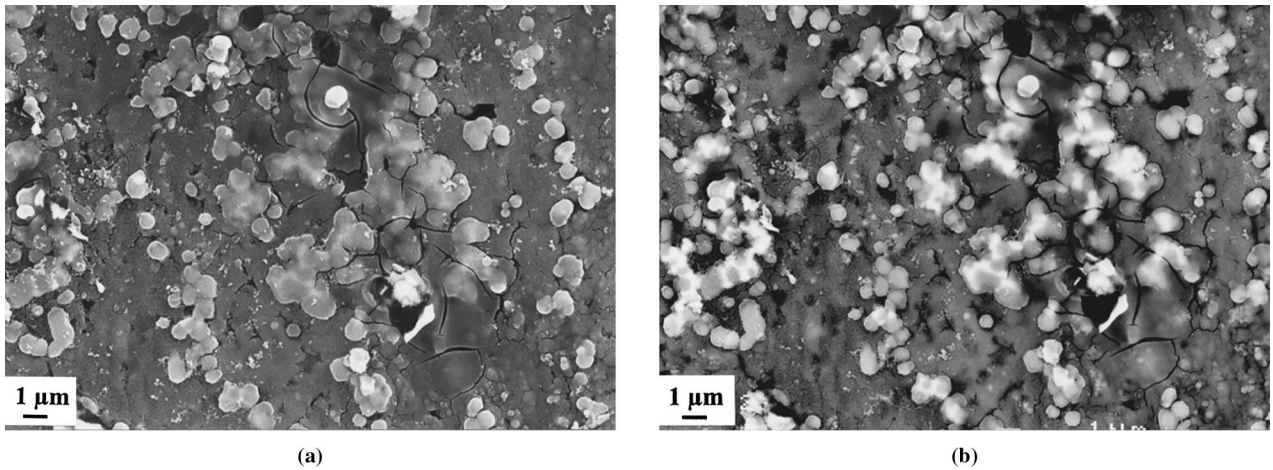

Figure 5 (a) Microstructure of the composite weld with signal of whisker dissolution and formation of intermetallic phases in the matrix. (b) BSE image.

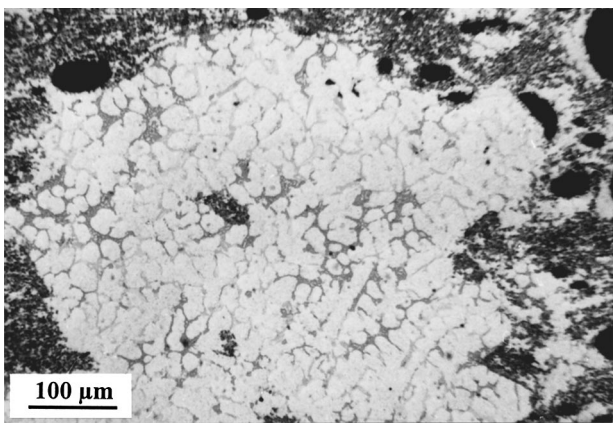

Figure 6 SiCw redistribution inside the weld with formation of large free-reinforcement zones.

pores. Their inner surfaces show the presence of tabular aggregates with hexagonal morphologies associated with the partially dissolved whiskers, although not always nucleated on them (Fig. 7a). EDX microanalysis of these tabular phases identified them as aluminium carbide (Fig. 7b).

However, the most drastic microstructural changes were observed at the top of the weld, because of the higher temperatures reached there. In this zone there is complete dissolution of the SiC whisker with the formation of a complex microstructure consisting of two different types of carbides and other Si-rich eutectic structures. The BSE image of the top-weld microstructure (Fig. 8a) shows the formation of two kinds of needle aggregate, which are easily distinguished by their different average atomic numbers. EDX microanalysis (Fig. 8b and c) show that both are aluminium carbide compounds, although the heavier one (brighter one) is richer in Si; the darker needles have a higher proportion of oxygen.

A detailed study of both kinds of carbide successfully differentiated their microstructure and properties. Si-rich aluminium carbide forms wider platelets, which are usually bonded to make up a continuous structure (Fig. 9a). The matrix that surrounds them is formed by Al-Al_2Cu eutectic aggregates, although a minority Si-Mg-Al-Cu eutectic phase was also detected (Fig. 9b and c). The other carbide has long-flake forms presenting a high level of chemical alteration, which is distinguished by preferential dissolution which develops an inner exfoliate structure (Fig. 10a and b). The nucleation of a eutectic phase was also detected in these aggregates, in this case the Si-Mg rich phase.

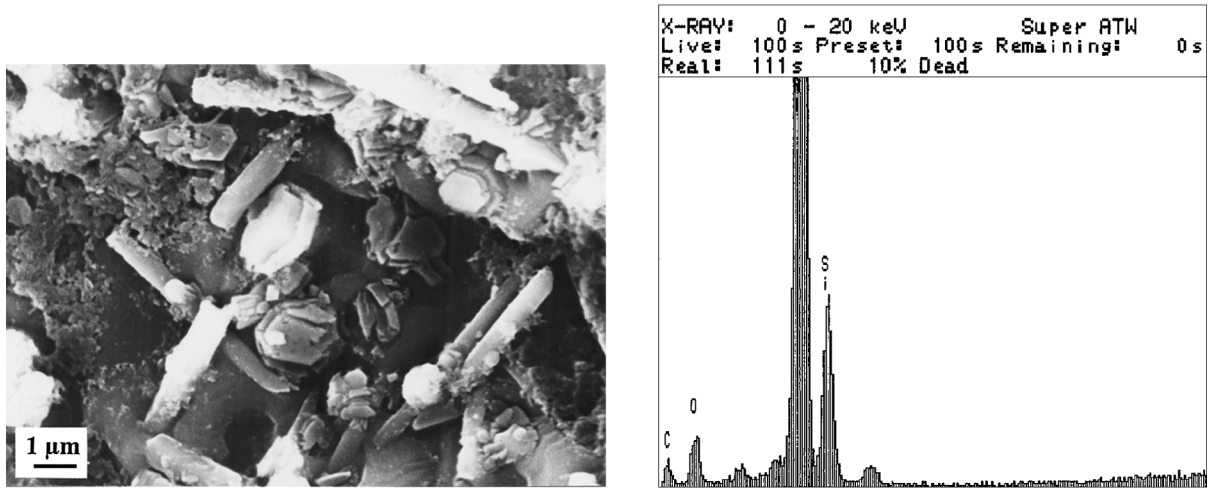

(a) (b)

Figure 7 (a) Al_4C_3 tabular crystals associated to SiC whiskers inside a pore formed during solidification. (b) EDX microanalysis of Al_4C_3 crystals.

The comparative study of both kinds of carbides formed showed clear differences in relation to both their chemical and their mechanical behaviour. The aluminium carbide with Si did not present the characteristic chemical alteration with humidity of the Al_4C_3. Hydration of the aluminium carbide was accompanied by an increase in volume, which even caused deformation of the surrounding aluminium matrix. This effect was not observed in the Al-Si carbides in spite of their remaining in a wet environment for long times. The other clear difference between the two reaction carbides was their respective hardness. Vickers microhardness measurements carried out on zones where each type of carbide was predominant gave very different values: 1200 HV for Si-rich aluminium carbide and 250–300 HV for Al_4C_3.

Complete identification of both types of carbides was only possible by TEM-ED. Fig. 11 shows a Al_4C_3 crystal which was identified ED. Inside the carbide crystal is a banded structure which may have originated from stacking faults occurring during the crystal growth. The aluminium alloy which surrounds the carbide exhibits precipitation of hardening phases with a preferential orientation visible when the matrix is orientated with the $[01\bar{1}]$ axis zone (Fig. 12a). Fig. 12b shows a dark field detail of these orientated precipitates whose composition corresponds to the hardening phase Al_2CuMg.

The second kind of carbide formed by the reaction of SiC and molten aluminium at the highest temperatures of the molten pools was identified by TEM-ED as β-Al_4SiC_4 (whose formation according to other investigators is only possible at temperatures higher than 1650 K) from Al-SiC mixtures [12]. Fig. 13 shows a TEM micrograph of one of these ternary carbide crystals, which is nucleated on the surface of a larger Al_4C_3 flake. The ED on the crystal confirms that it is the hexagonal β-Al_4SiC_4 diffracted along its $[\bar{1}2\bar{1}0]$ zone axis.

Fig. 13 also confirms the higher susceptibility of the longer Al_4C_3 flakes to wet degradation, showing the unaltered crystal of β-Al_4SiC_4 included in an amorphous surface layer of Al-O created on a Al_4C_3 flake.

TEM-ED also successfully identified interface reaction products such as elementary Si, mainly present as globular aggregates, which usually nucleate on the aluminium carbides (see Fig. 14). The globulized form of these crystals is associated with the overheating undergone by the molten pool, especially in the top zone of the arc discharge. Complex Si-rich eutectic aggregates were also identified in this upper zone; Fig. 15 shows a TEM image of one of these, in this case the quaternary $Al_{1.9}CuMg_{4.1}Si_{3.3}$ phase. More minority Al-Fe-Si intermetallic phases (Fig. 16a and b), with needle morphologies were also found.

4. Discussion

The combination of higher temperatures reached in the molten pools during the arc discharge (<2000 K) and high heating and cooling rates, modified the reactivity between whiskers and the molten matrix, originating different microstructures from those generated during conventional casting procedures.

The main microstructural differences observed when rapid welding cycles were applied on SiC whiskers reinforced aluminium alloys as follows.

4.1. Formation of a zone with complete dissolution of reinforcement

For all the experimental welding conditions, the high temperatures reached in the arc discharge zone produced a narrow band where all the reinforcement had disappeared. This zone, whose depth depends on welding power, had a complex microstructure where the formation of two reaction products between the matrix and the reinforcement was detected: Al_4C_3 and Al_4SiC_4. Both aggregates were characterised by needle shapes, although there were important differences, not only in their morphologies and structures, but also in their mechanical strength and chemical resistance, as described in the results.

The formation of Al_4C_3 in this zone cannot be explained independently from the generation of ternary

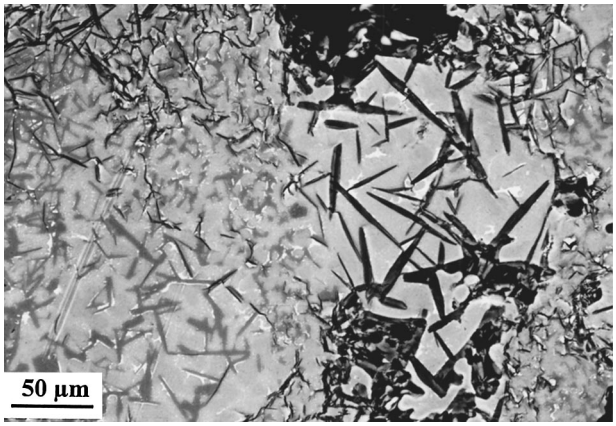

(a)

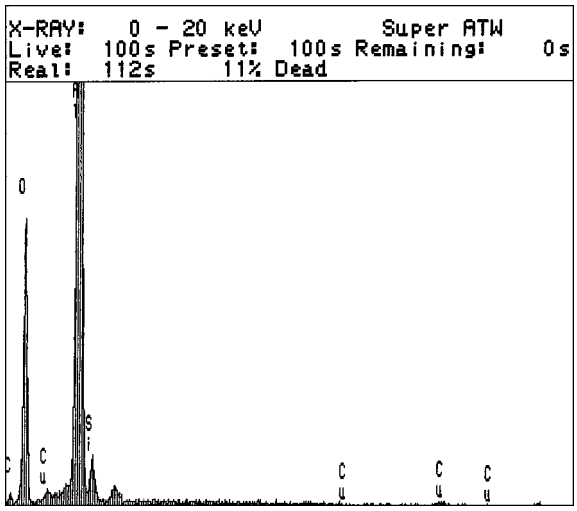

(b)

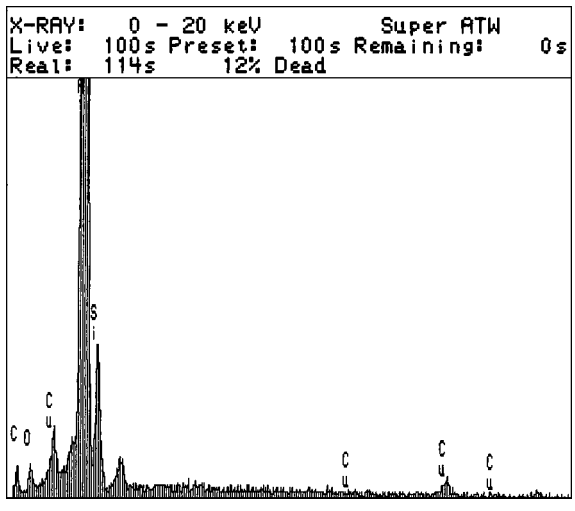

(c)

Figure 8 (a) Formation of two kind of carbide needles in the top of a weld, BSE image. (b) EDX of the lighter phase (Al_4C_3). (c) EDX of the heavier phase (Al_4SiC_4).

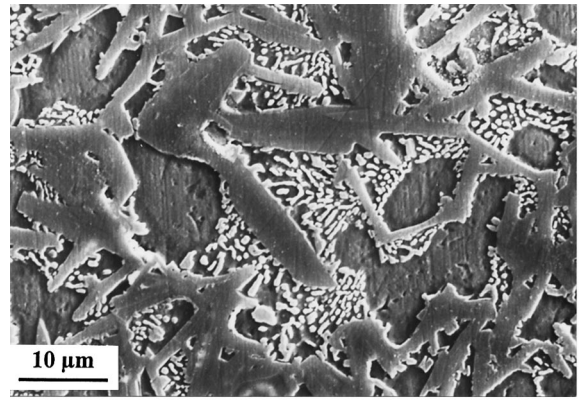

(a)

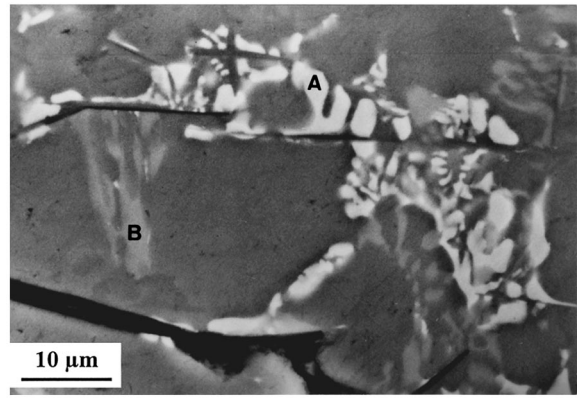

(b)

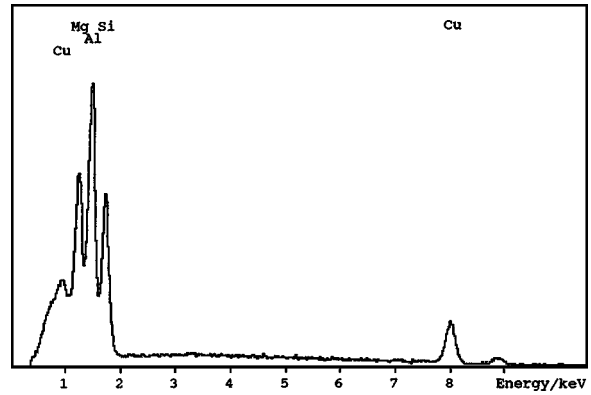

(c)

Figure 9 (a) Si-rich aluminium carbides with an eutectic structure nucleated on them. (b) BSE image of two kind of eutectic aggregates: Al_2Cu (marked with A) and Si-Mg-Al-Cu (marked with B). (c) EDX of the minority intermetallic (B).

carbide. The reaction between aluminium and silicon carbide is thermodynamically possible at temperatures higher than 650 °C, following the reaction (1) to generate Al_4C_3 and Si. This equilibrium is the predominant one in a temperature range of 650–1350 °C. When a mixture of Al-Si-C is subjected to temperatures between 1350 and 1625 °C to form a homogeneous liquid phase, as occurs inside the top of an arc weld, two monovariant equilibria may be reached depending on the liquid phase composition [9, 12].

$$\text{Stable equilibrium:} \quad L' \leftrightarrow Al_4\,SiC_4 + SiC \quad (3)$$

$$\text{Metastable equilibrium:} \quad L'' \leftrightarrow Al_4\,SiC_4 + Al_4\,C_3 \quad (4)$$

If the mixture reached temperatures higher than 2000 °C, the metastable equilibrium (4) would be substituted by two stable equilibria which would originate a second type of ternary carbide (Al_8SiC_7 or $2Al_4C_3{\cdot}SiC$). However, this compound was not detected for the welding conditions tested in the present work.

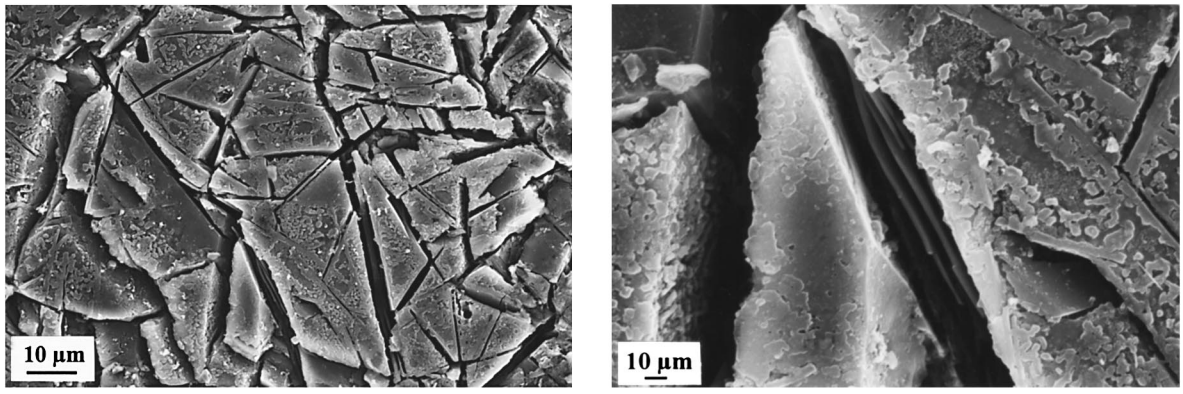

Figure 10 (a) Partial dissolved Al_4C_3 flakes by humidity action. (b) Detail at higher magnifications.

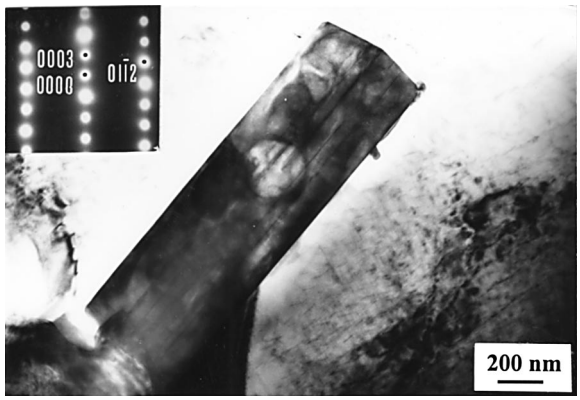

Figure 11 TEM image of an Al_4C_3 crystal growing in the Al matrix (ED pattern of Al_4C_3).

The formation of Al_4SiC_4 ($Al_4C_3{\cdot}SiC$) responds to the following stequiometric chemical reaction:

$$4Al + 4SiC \rightarrow Al_4SiC_4 + 3Si \qquad (5)$$

This reaction cannot be completed when the initial mixture has more than 40% mol of SiC. On the other hand, if it has less than 10% mol, everything is transformed into Al_4SiC_4 and Al_4C_3 [12].

From these data it can be established that the thermal action of the electric arc, working in direct current mode (with the composite sheet connected to the positive pole of the power source), forms a homogeneous Al-Si-C liquid phase (by complete dissolution of the whisker in the molten Al). The formation of the two kinds of carbide detected occurred by joint precipitation from this liquid phase. The characteristic morphology of the Al_4C_3 needles (showing curved shapes) demonstrates that this phase was formed from a turbulent pool.

Once both carbides have precipitated, the molten aluminium continues being Si-rich. During the subsequent cooling, the formation of Si-rich eutectic aggregates ($Al_{1.9}CuMg_{4.1}Si_{3.3}$ and free Si) occurred mainly by nucleating on the needle carbide surfaces.

Another significant fact to be considered is that this SiC free zone usually solidifies with a complete absence of porosity, which was not the case in the rest of the weld. That is because this zone had its origin in a homogeneous liquid phase, which probably possessed high fluidity due to the absence of ceramic phases.

4.2. Porosity formation due to wettability problems

With the exception of the weld top, most of the solidified pools were characterised by a high level of porosity occurring during melting. This effect is associated with

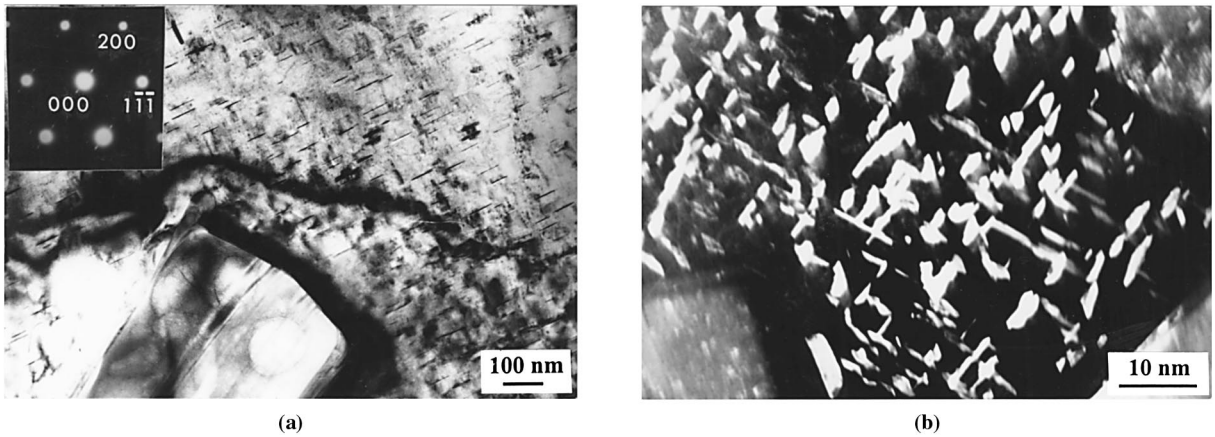

Figure 12 (a) Detail of the matrix surrounding the Al_4C_3 crystal with hardener Al_2MgCu precipitates. (b) Dark field image showing the preferential orientation of those precipitates following the $[01\bar{1}]_{Al}$ axe.

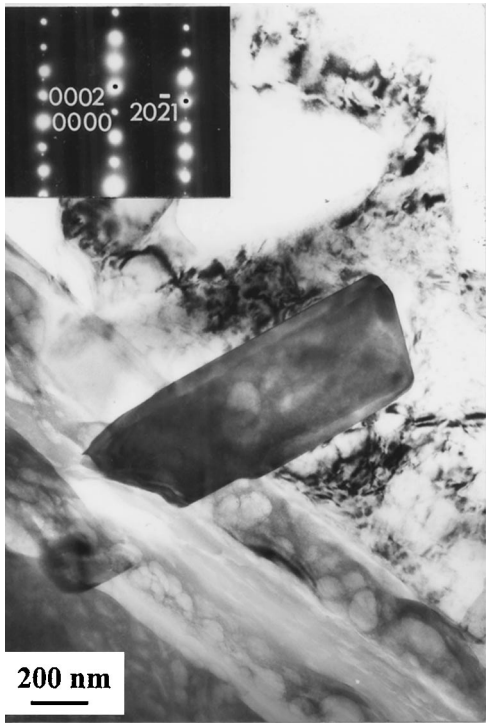

Figure 13 TEM image of a β-Al_4SiC_4 crystal identified by electron diffraction.

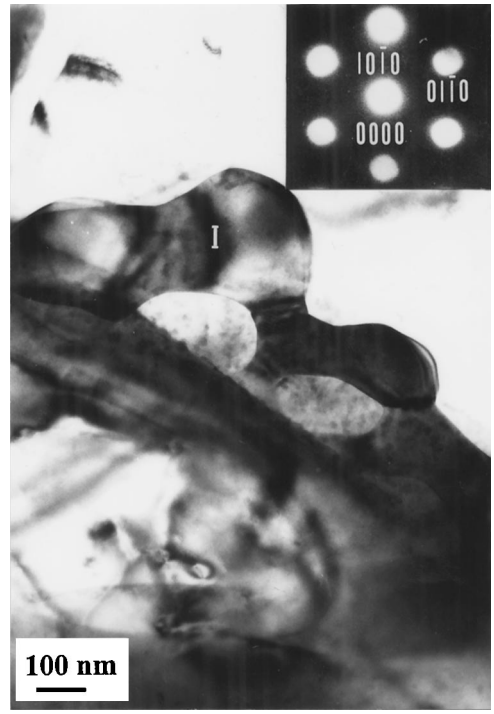

Figure 15 TEM image of the quaternary $Al_{1.9}CuMg_{4.1}Si_{3.3}$ eutectic aggregate (marked with I) identified by ED.

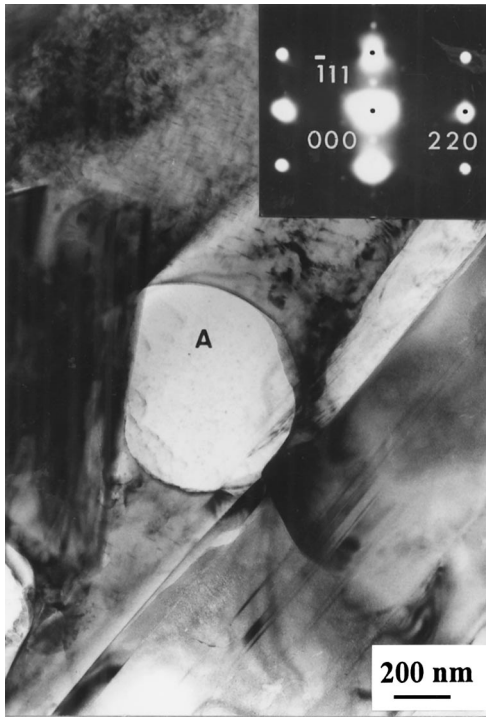

Figure 14 TEM image of Si aggregates (marked with A) with globular morphologies, including its ED pattern.

the low wettability of the SiC by molten aluminium. Although this kind of behaviour also occurs in conventional casting procedures, it is more accentuated during welding, for the following reasons:

– The high rates during the thermal cycles applied during welding inhibit the interface reaction between Al and SiC, sensitively limiting the formation of plated Al_4C_3 aggregates on the Al/SiC*w* interface. Although the formation of this compound is detrimental to composite properties; the participation of a interface reaction during wetting always increase wettability.

– The increase of interface energy produced by the fact that the Al/SiC reaction is not kinetically favoured, causes the solidification front to push the ceramic whiskers. This phenomenon favours the formation of zones with a high proportion of ceramic reinforcement, producing discontinuities inside the welds. It can even occur during the melting of the composites, causing raising of the molten pool. This is not simply a case of gaseous porosity or contraction cavities but is primarily a serious weldability problem which could produce hot cracking.

4.3. Formation of platelet Al_4C_3

Although the formation of the typical hexagonal platelet of Al_4C_3 inside the welds is kinetically inhibited, this does not mean that its formation is completely ruled out. However, it is less favoured than in conventional casting procedures carried out at lower temperatures (725–900 °C) for longer times (15–30 min) [13]. Besides, the Si enrichment of the aluminium matrix that surrounds the whiskers inside the weld is noticeably lower. Si lakes formed by isothermal solidification around whiskers during casting were not detected in welded specimens, although there was some slight Si enrichment which produced the precipitation of Si-rich eutectic aggregates combined either with Al or with other alloying elements (Cu, Mg, Fe). Agitation of the molten pool during the arc discharge favoured more homogeneous distribution of the Si aggregates inside the welds.

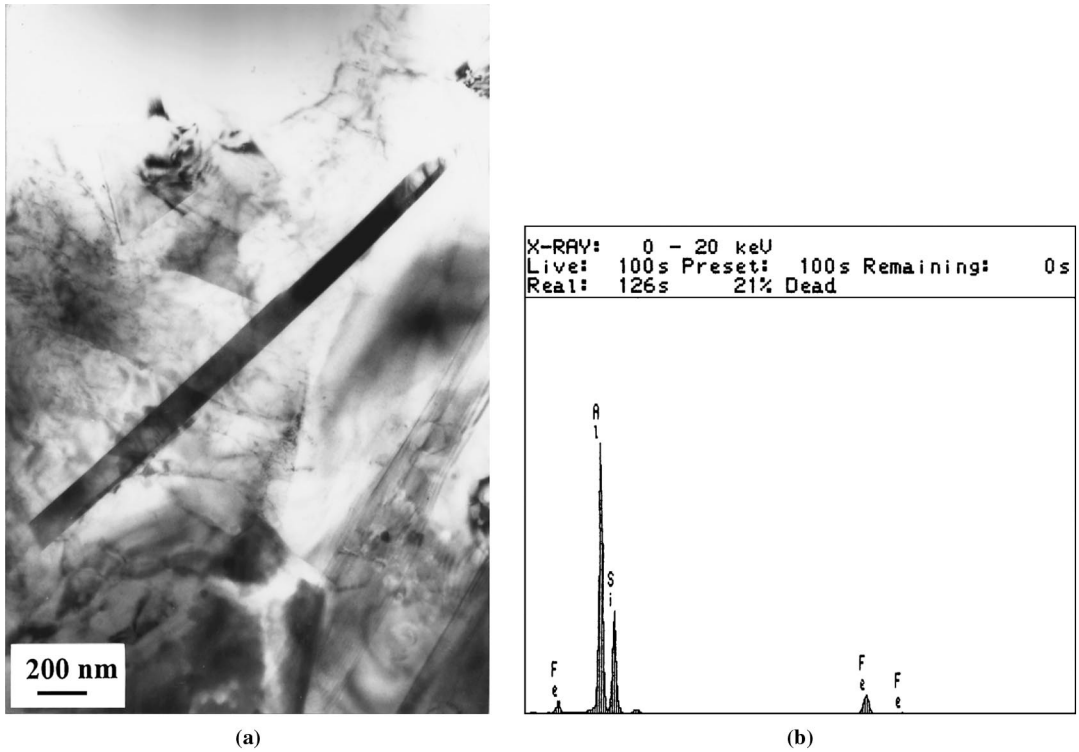

(a) (b)

Figure 16 Al-Fe-Si intermetallic with needled morphology detected in the aluminium matrix composite. (b) EDX microanalysis of the needle.

4.4. Chemical and mechanical characteristics of the interface reaction products

Besides the intermetallic compounds generated in the aluminium matrix due to Si enrichment by dissolution of whiskers, the main difference observed between reactivity in a SiC whisker reinforced aluminium composite under conventional melting conditions (casting) and reactivity with higher-energy and faster melting conditions (welding), was the formation of a ternary carbide identified as β-Al_4SiC_4. The results showed that this reaction compound had higher strength (hardness) than the Al_4C_3 and, more importantly, less tendency to hydration. Long flakes of Al_4C_3 underwent rapid etching in wet environments, generating amorphous Al-O compounds entailing considerable strain on the aluminium matrix because of increasing volume during hydration (reaction (6)) [14].

$$Al_4C_3 + 18H_2O \rightarrow 4Al(OH)_3 + 3CO_2 + 12H_2 \quad (6)$$

Even after only a few days in contact with wet environments, Al_4C_3 flakes located on the specimen surface dissolved completely. However, the β-Al_4SiC_4 was not altered in any way, even those crystals which nucleated in contact with the altered Al_4C_3 flakes.

Its greater hardness and greater chemical resistance suggests that β-Al_4SiC_4 could be used as a thermally and chemically stable reinforcement in aluminium alloys. Although its formation along with Al_4C_3 during arc welding of SiC whisker reinforced aluminium composites degrades the material, synthesis from a mixture of SiC*w* and Al by arc melting, followed by extraction from the rest of the reaction products, could provide a new kind of reinforcement for aluminium alloys.

5. Conclusions

1. The high energy conditions produced during arc welding (TIG) of an aluminium matrix composite reinforced with SiC whiskers favoured the formation of a zone where the complete dissolution of reinforcement occurred, jointly the formation of two kinds of needled carbides: Al_4C_3 and β-Al_4SiC_4.

2. The ternary carbide β-Al_4SiC_4 has higher hardness and behaves better in a wet environment than the Al_4C_3, which suggests that this carbide might be applicable as a thermally and chemically stable reinforcement in aluminium matrices.

3. The main problem with weldability of SiC whisker reinforced aluminium composites is not the interface reactivity, but mainly the low wettability of this kind of reinforcement, which is aggravated by its high aspect ratio (specific surface). This low wettability produces a pushing effect that causes the whiskers to accumulate in the solidification front, creating metallic discontinuity (porosity or hot cracking).

Acknowledgements

The authors wish to thank the *Comisión Interministerial de Ciencia y Tecnología (CICYT)* for the financial support provided to this research (Project MAT97/0719).

References

1. A. UREÑA, J. M. GÓMEZ DE SALAZAR and M. D. ESCALERA, *Key Eng. Mat.* **104–107** (1995) 523.
2. A. UREÑA, J. M. GÓMEZ DE SALAZAR, L. GIL, M. D. ESCALERA and J. L. BALDONEDO, *J. Microscopy.* **196** (1999) 124.
3. M. B. D. ELLIS. *Int. Mat. Rev.* **41** (1996) 41.
4. C. T. LANE, "ASW Welding Handbook, Vol. 3" (American Welding Society, 1994).
5. J. A. AHEARN, C. COOKE and S. G. FISHMAN. *Met. Constr.* **14** (1982) 192.

6. T. J. LIENERT, E. D. BRANDON and J. C. LIPPOLD, *Script. Met. Mat.* **28** (1993) 1341.
7. DURALCAN®, "Composites Arc Welding Guidelines" (Duralcan, San Diego CA, USA, 1991).
8. D. S. SHIN, J. C. LEE, E. P. YOON and H. I. LEE, *Mater. Res. Bull.* **32** (1997) 1155.
9. J. C. VIALA, P. FORTIER and J. BOUIX, *J. Mater. Sci.* **25** (1990) 1842.
10. A. S. ISAIKIN, V. M. CHUBAROV, B. F. TRETILOV, V. A. SILAEV and Y. A. GORELOV, *Met. Sci. Heat Treat. (Russia)* **22** (1980) 815.
11. M. B. D. ELLIS, M. F. GITTOS and P. L. THREADGILL, "Joining of Aluminium Based Metal Matrix Composites: Initial Studies" (TWI , Members Reports No. 501, Abington, UK, 1994).
12. L. D. ODEN and R. A. MCCUNE, *Met. Trans. A.* **26A** (1987) 2005.
13. A. UREÑA, P. RODRIGO, L. GIL, M. D. ESCALERA and J. L. BALDONEDO. *J. Mater. Sci.* **36** (2001).
14. J. K. PARK and J. P. LUCAS, *Script. Mat.* **37** (1997) 511.

Received 25 October 1999
and accepted 2 May 2000